Modeling and Identification Approach for Tripod Machine Tools

Shi Yong(石勇)[1*], *Liu Wentao*(刘文涛)[2]

1. College of Power and Energy Engineering, Harbin Engineering University, Harbin 150001, P. R. China;
2. School of Mechatronic Engineering, Harbin Institute of Technology, Harbin 150001, P. R. China

(Received 4 November 2014; revised 24 December 2014; accepted 25 March 2015)

Abstract: To improve stiffness and workspace of tripod machine tools, a device called tripod machine tool was proposed with five degrees of freedom. First, the structure and pose description of the tripod machine tool were introduced, and then its backward and forward kinematics models were analyzed. To identify parameters of the tripod machine tool, a parameter identification method based on an error-sensitive analysis was presented. Then geometrical structural identification model was deduced by establishing the pose relative error model at two different points of the tripod machine tool. The method employed a sensitivity matrix by using a difference operator to explain pose changes of the tripod machine tool with respect to its main geometrical structural parameters. Finally, the position error of a tripod machine tool was reduced from 1.74 mm to 0.44 mm. Therefore, the proposed identification method was verified to be effective and feasible.

Key words: tripod; error sensitivity analysis; calibration; identification

CLC number: TG659 **Document code:** A **Article ID:** 1005-1120(2015)06-0665-09

0 Introduction

To improve stiffness and workspace of Tripod machine tools, a series-parallel hybrid machine tool called tripod was proposed, as shown in Fig. 1. The parallel part of the tool was comprised a base platform, a moving platform, and three legs with adjustable lengths. One end of each leg was connected to the moving platform by a revolute pair, and the other end of two was connected to the base platform by Hooke joints; the third leg was connected to the base platform by a ball joint or Hooke joint with three degrees of freedom (DOFs). The parallel part of the tripod machine tool has three DOFs. The motion parameters of the parallel part have coupling characteristics. The position parameters of the tripod machine tool are independent from each other, but the orientation parameters are calculated with those position parameters. To increase the flexibility of the tripod machine tool, two perpendicular rotary shafts were installed under the moving platform in series, which has two DOFs.

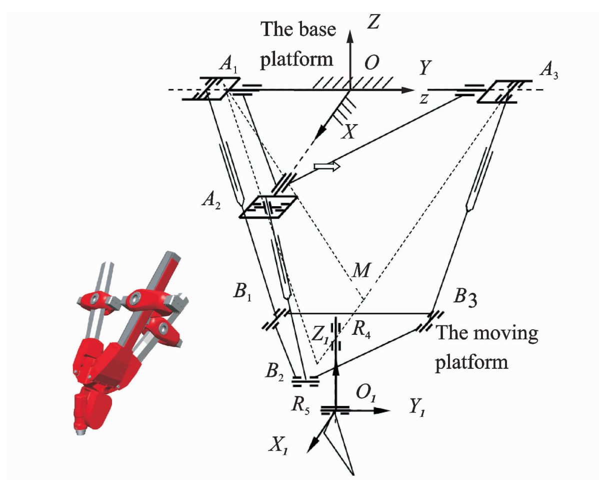

Fig. 1 Tripod machine tool

Accuracy of the tripod machine tool is inevitably affected by manufacturing and installation errors inevitably. Therefore, tripod machine tools must be calibrated before application. In general, calibration methods can be classified into three

* **Corresponding author:** Shi Yong, Associate Professor, E-mail: sy_hit@163.com.

How to cite this article: Shi Yong, Liu Wentao. Modeling and identification approach for tripod machine tools [J]. Trans. Nanjing U. Aero. Astro., 2015,32(6):665-673.
http://dx.doi.org/10.16356/j.1005-1120.2015.06.665

types: External calibration, constrained calibration, and auto-calibration or self-calibration[1]. Self-calibration requires internal sensors. Usually, the number of internal sensors is larger than that of DOFs of calibrated mechanisms[2-3]. Constrained calibration is implemented by constraining some of DOFs of the calibrated mechanisms and keeping some geometric parameters constant throughout the whole process. Constrained calibration does not require extra sensors[4]. External calibrations neither require additional internal sensors nor restrict some of the DOFs of calibrated mechanisms. The position and orientation information of calibrated mechanisms are obtained using external measuring devices, such as a laser tracker, an inclinometer, or a coordinate measuring maching (CMM). This calibration method has been widely used[4-8].

Recent literature have reported identification model of parallel machine tools (PKM). Based on PKM forward kinematics model, Ref. [9] constructed an influence coefficient matrix with the pose errors and structure errors of PKM by a numerical method using measured data. A min-max optimization method was presented in Ref. [10] based on the least square optimization method to eliminate a few large residual errors that lie in the parameter identification. An experiment proved that the min-max optimization method directly correlated the precision evaluation with the kinematics calibration and improved the total accuracy of PKM tools simply and inexpensively. In Ref. [11], indirect measurements of the position and orientation of moving platform were performed using a photoelectric length gauge with balls. Since measuring noises caused final calculation results seriously to deviate from the real existing error values of the machine tool, Jacobian matrix regrouping method was presented to minimize magnification of measuring noises while identifying parameters. A so-called cocktail method was an example of it[12]. The structure error Jacobean matrix was automatically constructed based on the forward kinematics model, and generalized coordinates consistent with the measuring apparatus were adopted. The method can employ different types of common measuring apparatus or the combination of them when a Stewart platform is calibrated, thus so the special equipment for multi-freedom measurement is unnecessary. In Ref. [13], an error compensation method was designed to compensate for manufacturing and assembly error by developing a 3-point-3-axe measurement method so that position accuracy, and other attributes were improved.

Our work was to propose a structural characteristic and kinematic model for tripod machine tools. A parameter identification method was designed based on parameter error sensitivity matrix proposed. The method measured relative position and orientation error of tripod machine tools in different moving directions and different spaces. Then, we constructed a parameters error sensitivity matrix by using a numerical method. Combining the matrix and the relative pose error data, the geometrical structure parameters of tripod machine tools were identified. Our results showed that the method was convenient, practical and efficient.

1 Main Parameters of Tripod Machine Tool

As shown in Fig. 1, A_i ($i=1,2,3$) and B_i ($i=1,2,3$) are the joints of the base platform and the moving platform, respectively. A_iB_i ($i=1,2,3$) are the three legs with adjustable lengths. The rotary shaft S_4 (R_4, R_5) is perpendicular to the moving platform, and they intersect at point R_4. Rotary shafts S_5 and S_4 are perpendicular to each other, and their intersection is at point R_4. The base Cartesian coordinate system $\{O\}$, which is fixed on the base platform, is defined. In $\{O\}$, the origin O satisfies $A_1A_3 \perp OA_2$; X-axis is OA_2; and Y-axis is A_1A_3. The Cartesian moving coordinate system $\{O_1\}$, which is fixed on the moving platform, is defined. In $\{O_1\}$, the origin O_1 is at point R_5, Y_1-axis is B_1B_3; and Z_1-axis is R_5R_4.

The main geometrical parameters of the tripod machine tool are shown in Table 1. The parameters include position parameters of joints on the base platform, installing error of the joints on the base platform in the vertical direction, position coordinates of the joints on the moving platform, geometrical structure parameters of series part, etc. There are a total of 12 parameters. Fig. 2 shows a schematic of those parameters.

Table 1 Parameters of the tripod machine

Parameter	Geometric meaning
a_1	The distance between joint A_1 and the origin O
a_2	The distance between joint A_3 and the origin O
b	The distance between joint A_2 and the origin O
c_1	The distance between joint B_1 and the origin O_1 along Y_1-axis
c_2	The distance between joint B_3 and the origin O_1 along Y_1-axis
d	The distance between joint and the origin O_1 along Z_1-axis
d_1	The distance between joint B_2 and the origin O_1 along X_1-axis
d_2	The distance between joint $B_i(i=1,3)$ and the origin O_1 along X_1-axis
c	The offset between rotary shaft 5 and its nominal position
t_1	The offset between the tool axis and its nominal position
t_2	Length of the cantilever for the installing tool
t_3	Length of the tool

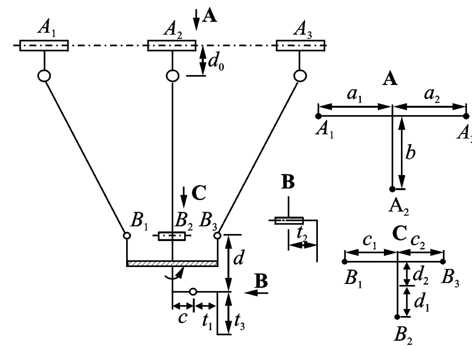

Fig. 2 Schematic of tripod platform parameters

3 Description of the Orientation of Moving Platform

Position and orientation of the moving platform of tripod machine tools can be described by moving the coordinates system $\{O_1\}$ relative to the base coordinates system $\{O\}$. Commonly, there are two ways to describe the orientation of the moving platform: Euler angle or RPY angle. Here, we describe the orientation of the moving platform using RPY angle. Hence, the transformation matrix from $\{O_1\}$ to $\{O\}$ is

$$\boldsymbol{T}=\begin{bmatrix}\cos\theta_z\cos\theta_y & \cos\theta_z\sin\theta_y\sin\theta_x-\sin\theta_z\cos\theta_x & \cos\theta_z\sin\theta_y\cos\theta_x+\sin\theta_z\sin\theta_x \\ \sin\theta_z\cos\theta_y & \sin\theta_z\sin\theta_y\sin\theta_x+\cos\theta_z\cos\theta_x & \sin\theta_z\sin\theta_y\cos\theta_x-\cos\theta_z\sin\theta_x \\ -\sin\theta_y & \cos\theta_y\sin\theta_x & \cos\theta_y\cos\theta_x\end{bmatrix}$$

In $\{O\}$, the pose of the moving platform can be written as $(x_{O_1}, y_{O_1}, z_{O_1}, \theta_x, \theta_y, \theta_z)$. Since the parallel part has 3-DOF, the parameters $(x_{O_1}, y_{O_1}, z_{O_1}, \theta_x, \theta_y, \theta_z)$ are not fully independent from each other. There are three constraint equations reflected in the mechanism structure and performance: (1) Plane $A_1A_3B_3B_1$, which is perpendicular to plane $B_1B_2B_3$; (2) $A_2B_2\perp A_1B_3$; (3) the moving platform cannot turn around axis R_4R_5, namely, $\theta_z=0$.

As shown in Fig. 1, define point M as the intersection of line B_2R_4 and B_1B_3, and draw lines A_1M, A_3M, A_1B_2, A_3B_2, and OM. It is obvious that $A_1A_3B_3B_1$ forms a plane four bar mechanism. Since line R_4M is perpendicular to plane $A_1A_3B_3B_1$, both $\triangle MA_1B_1$ and $\triangle MA_3B_2$ are right-angled triangles. Thus, the following equations can be obtained

$$\overrightarrow{MA_1}\cdot\overrightarrow{MB_2}=0 \tag{1}$$

$$\overrightarrow{MA_3}\cdot\overrightarrow{MB_2}=0 \tag{2}$$

According to definitions in Table 1, we have $R_4B_2=d_1$ and $R_4M=d_2$. Substitute them into Eqs. (1,2) and then add the two results in the following equation

$$\sin\theta_z\cos\theta_y=0 \tag{3}$$

Due to the structural constraint, $\theta_y\in(-90°, 90°)$. Hence, $\cos\theta_y\neq0$. From Eq. (3), the following equation can be obtained

$$\sin\theta_z=0 \tag{4}$$

By adding Eq. (1) and Eq. (2), θ_y can be obtained as

$$\begin{cases}\theta_y=2\arctan(d_2/z_{O_1}), & x_{O_1}=-d_2\\ \theta_y=2\arctan\left(\dfrac{-z_{O_1}-\sqrt{z_{O_1}^2+x_{O_1}^2-d_2^2}}{x_{O_1}+d_2}\right), & x_{O_1}\neq-d_2\end{cases} \tag{5}$$

In Fig. 1, because $B_1B_3 // A_1A_3$ and $A_1A_3 \perp OA_2$, thus $B_1B_2 \perp OA_2$. Since $B_1B_3 \perp MOA_2B_2$ and $B_1B_3 \perp A_2B_2$, the following equation can be obtained

$$\overrightarrow{B_1B_3} \cdot \overrightarrow{A_2B_2} = 0 \tag{6}$$

Substitute the geometrical structure, position, and orientation parameters into Eq. (6), θ_x can be expressed as

$$\theta_x = -\arctan\left(\frac{y_{O_1}}{(y_{O_1} - b)\sin\theta_y + z_{O_1}\cos\theta_y}\right) \tag{7}$$

Therefore, the three constraint equations in the parallel part are Eqs. (3,5,7).

In the series part of tripod machine tools, the description of motions can be expressed by angles θ_4 and θ_5 of the two rotary shafts S_4 and S_5.

3 Kinematics Model

3.1 Backward kinematics model the tripod machine tool

The backward kinematics model of tripod machine tools is used to calculate lengths $l_i (i=1, 2,3)$ of the three legs and angles θ_4 and θ_5 of the two rotary shafts, on the condition that the tool pose in $\{O\}$ is known.

3.1.1 Backward kinematics model of parallel part

The backward kinematics model of the parallelpart is used to calculate lengths $l_i (i=1,2,3)$ of the 3 legs with the knowledge of the tool pose in $\{O\}$. This calculation can be achieved in two steps as follows.

(1) Calculating the position coordinates of the moving platform

As shown in Fig. 3, another moving coordinates system $\{O_2\}$ is defined, which is fixed on the series part of the tripod machine tool, with the tool center point as the origin O_2, the tool axis $\overrightarrow{O_2K_1}$ as Z_2-axis, and $\overrightarrow{K_1K_2}$ as Y_2-axis.

In $\{O\}$, assume that the position and orientation coordinates of the tool are described as $(x, y, z, \alpha, \beta, \gamma)$, where x, y, z are the position coordinates of the tool center point, and α, β, γ are Euler angle orientation coordinates of the tool. The transformation matrix of Euler angles can be written as $\boldsymbol{T}_{\text{sm}} = T(Z, \alpha) T(Y, \beta) T(Z, \gamma)$, namely

$$\boldsymbol{T}_{\text{sm}} = \begin{bmatrix} \cos\alpha\cos\beta\cos\gamma - \sin\alpha\sin\gamma & -\cos\alpha\cos\beta\sin\gamma - \sin\alpha\cos\gamma & \cos\alpha\sin\beta \\ \sin\alpha\cos\beta\cos\gamma + \cos\alpha\sin\gamma & -\sin\alpha\cos\beta\sin\gamma + \cos\alpha\cos\gamma & \sin\alpha\sin\beta \\ -\sin\beta\cos\gamma & \sin\beta\sin\gamma & \cos\beta \end{bmatrix}$$

In $\{O_2\}$, the vector $\overrightarrow{O_1O_2}$ can be expressed as

$$\overrightarrow{O_1O_2} = \overrightarrow{O_2K_1} + \overrightarrow{K_1K_2} + \overrightarrow{K_2K_3} + \overrightarrow{K_3O_1} \tag{8}$$

After coordinate transformation, in $\{O_2\}$, there is

$$\boldsymbol{O}_1 = \boldsymbol{T}_{\text{sm}} \cdot \overrightarrow{O_1O_2} + \boldsymbol{O}_2$$

Namely

$$\begin{vmatrix} x_{O_1} \\ y_{O_1} \\ z_{O_1} \end{vmatrix} = \begin{bmatrix} x - t_1(s\gamma\zeta\alpha + s\alpha s\beta\zeta\gamma) + (t_2 + c \cdot s\theta_5)(\zeta\alpha\zeta\gamma - s\alpha s\beta s\gamma) + s\alpha\zeta\beta(t_3 + c \cdot \zeta\theta_5) \\ y + t_1(s\gamma s\alpha - \zeta\alpha s\beta\zeta\gamma) - (t_2 + c \cdot s\theta_5)(s\alpha\zeta\gamma + \zeta\alpha s\beta s\gamma) + \zeta\alpha\zeta\beta(t_3 + c \cdot \zeta\theta_5) \\ z + s\beta(t_3 + c \cdot \zeta\theta_5) + s\gamma\zeta\beta(t_2 + c \cdot s\theta_5) + t_1\zeta\beta\zeta\gamma \end{bmatrix} \tag{9}$$

where s denotes the trigonometric function cos, and ζ the trigonometric function sin.

In $\{O\}$, when the position coordinates $(x_{O_1}, y_{O_1}, z_{O_1})$ of the origin O_1 are known, the orientations θ_x, θ_y, θ_z of $\{O_1\}$ can be calculated from Eqs. (3, 5, 7).

(2) Calculating the lengths of three the legs

According to the definition in Table 1, the position coordinates of the joints $\boldsymbol{A}_i (i=1, 2, 3)$ are $\boldsymbol{A}_1 = [0 \quad -a_1 \quad 0]^{\text{T}}$, $\boldsymbol{A}_2 = [0 \quad a_2 \quad 0]^{\text{T}}$, $\boldsymbol{A}_3 = [b \quad 0 \quad 0]^{\text{T}}$ in $\{O\}$, respectively. The position

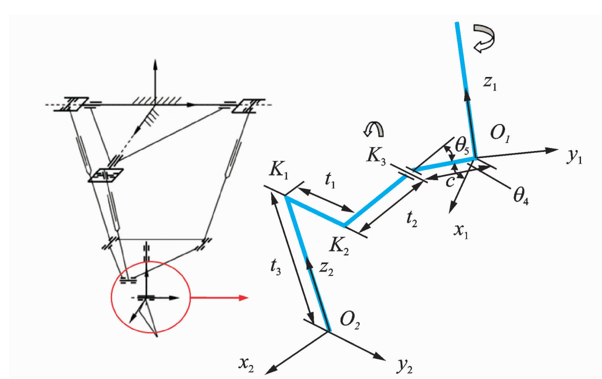

Fig. 3 Schematic of serial structure for analysis

coordinates of joints $\boldsymbol{B}_i (i=1, 2, 3)$ are $\boldsymbol{B}'_1 =$

$[-d_2 \quad -c_1 \quad d]^{\mathrm{T}}$, $\boldsymbol{B}'_2=[-d_2 \quad -c_2 \quad d]^{\mathrm{T}}$ and $\boldsymbol{B}'_3=[d_1 \quad 0 \quad d]^{\mathrm{T}}$ in $\{O_1\}$, respectively.

After coordinate transformation, the position coordinates of joint are expressed as

$$\boldsymbol{B}_i=\boldsymbol{T}\cdot\boldsymbol{B}'_i+\boldsymbol{O}_1 \quad i=1,2,3$$

Thus, the lengths of the three legs are

$$l_i=\|\boldsymbol{A}_i-\boldsymbol{B}_i\| \quad i=1,2,3 \tag{10}$$

3.1.2 Backward kinematics model of the series part

The backward kinematics model of the series part is used to calculate angles θ_4 and θ_5 of the two rotary shafts with knowledge of the tool pose in $\{O\}$.

In $\{O_2\}$, the orientation coordinates of the rotary shaft can be expressed as

$$\boldsymbol{n}_4^2=[\cos\theta_5 \quad 0 \quad \sin\theta_5]^{\mathrm{T}}$$

After coordinate transformation of $\boldsymbol{n}_4^2$, in $\{O\}$, the orientation coordinates of shaft S_4 are expressed as

$$\boldsymbol{n}_4=\boldsymbol{T}_{\mathrm{sm}}\boldsymbol{n}_4^2 \tag{11}$$

In the same way, in $\{O_1\}$, the orientation coordinates of the rotary shaft S_4 is expressed as

$$\boldsymbol{n}_4^1=[0 \quad 0 \quad 1]^{\mathrm{T}}$$

After coordinate transformation of $\boldsymbol{n}_4^1$, in $\{O\}$, the orientation coordinates of rotary shaft S_4 are expressed as

$$\boldsymbol{n}_4=\boldsymbol{T}\boldsymbol{n}_4^1=[\sin\theta_y\cos\theta_x \quad -\sin\theta_x \quad \cos\theta_y\cos\theta_x] \tag{12}$$

Since Eq. (11) is equal to Eq. (12), by using Eqs. (5, 7, 9), trigonometric equations for θ_5 can be created. An explicit solution to the equations is difficult to obtain, but the equations can be solved using a numerical iteration algorithm.

Define the orientation coordinates of the vector $\overrightarrow{O_1K_3}$ as $\boldsymbol{n}^2(O_1K_3)$ in $\{O_2\}$. After coordinate transformation, in $\{O_1\}$, the vector can be expressed as $\boldsymbol{n}(\overrightarrow{O_1K_3})=\boldsymbol{T}^{-1}\boldsymbol{T}_{\mathrm{sm}}\boldsymbol{n}^2(\overrightarrow{O_1K_3})$. Hence

$$\theta_4=a\tan\left[\frac{\boldsymbol{n}(\overrightarrow{O_1K_3})_y}{\boldsymbol{n}(\overrightarrow{O_1K_3})_x}\right] \tag{13}$$

3.2 Forward kinematics model of the tripod machine tool

The forward kinematics model of the tripod machine tool is used to calculate the position of the tool center point and orientation of the tool, on the condition of the lengths $l_i\,(i=1,2,3)$ of three legs and the angles of two rotary shafts are known.

3.2.1 Forward kinematics model of the parallel part

Using knowledge of the lengths of 3-legs to calculate the position and orientation of the moving platform is called the forward kinematics model of the moving platform.

From Eqs. (3, 5, 7), one obtains that θ_x, θ_y, θ_z are functions of x_{O_1}, y_{O_1}, and z_{O_1}, respectively. Therefore, the transformation matrix $\boldsymbol{T}$ is also a matrix of x_{O_1}, y_{O_1}, and z_{O_1}. With Eq. (10), equations for three unknown $x_{O_1}, y_{O_1}, z_{O_1}$ can be created. The results of the equations are difficult to calculate, but a numerical iteration algorithm can be used to solve them.

After the positions $x_{O_1}, y_{O_1}, z_{O_1}$ of the moving platform are solved, the orientation $\theta_x, \theta_y, \theta_z$ of the moving platform can be determined using Eqs. (3, 5, 7).

3.2.2 Forward kinematics model of the series part

The forward kinematics model of the series part involves calculation of the position and orientation of the tool on the condition of knowing the position and orientation coordinates of the moving platform and angles θ_4 and θ_5 of the two rotary shafts.

In Fig. 3, the matrix transforming $\{O_2\}$ into $\{O_1\}$ is

$$\boldsymbol{T}_{21}=\begin{bmatrix}-\cos\theta_5\cos\theta_4 & \sin\theta_4 & \sin\theta_5\cos\theta_4\\ -\cos\theta_5\sin\theta_4 & \cos\theta_4 & \sin\theta_5\sin\theta_4\\ \sin\theta_5 & 0 & \cos\theta_5\end{bmatrix}$$

Hence, in $\{O\}$, the tool center point $\boldsymbol{O}_2$ is

$$\boldsymbol{O}_2=\boldsymbol{O}_1+\boldsymbol{T}\boldsymbol{T}_{21}[t_2+c\cdot\cos\theta_5 \quad -t_1 \quad -c\cdot\sin\theta_5-t_3]^{\mathrm{T}} \tag{14}$$

The orientation coordinates of the vector $\overrightarrow{O_2K_1}$ are

$$\boldsymbol{n}(\overrightarrow{O_2K_1})=\boldsymbol{T}\boldsymbol{T}_{21}[0 \quad 0 \quad 1]^{\mathrm{T}} \tag{15}$$

The Euler angle orientation of the tool can be written as

$$\alpha=a\tan\left[\frac{\boldsymbol{n}(\overrightarrow{O_2K_1})_y}{\boldsymbol{n}(\overrightarrow{O_2K_1})_x}\right] \tag{16}$$

$$\beta=a\cos[\boldsymbol{n}(\overrightarrow{O_2K_1})_z] \tag{17}$$

Angle γ is not important to the machining.

Commonly, $\gamma=-\alpha$.

4 Identification Approach of Tripod Machine Tools

4.1 Parameter error analysis and parameter identification

Assume that $\boldsymbol{\theta}=[\theta_1\ \theta_2\cdots\ \theta_{12}]^{\mathrm{T}}$ denotes the 12 nominal geometrical structure parameters of tripod machine tools. When moving the machine tools from position $\boldsymbol{P}_1=[x_1\ y_1\ z_1\ \alpha_1\ \beta_1\ \gamma_1]^{\mathrm{T}}$ to position $\boldsymbol{P}_2=[x_2\ y_2\ z_2\ \alpha_2\ \beta_2\ \gamma_2]^{\mathrm{T}}$, we can determine the lengths of the three legs and angles θ_4 and θ_5 from the feedback of the servo motors, which change from $\boldsymbol{L}_1=[l_{11}\ l_{21}\ l_{31}\ \theta_{41}\ \theta_{51}]$ to $\boldsymbol{L}_2=[l_{12}\ l_{22}\ l_{32}\ \theta_{42}\ \theta_{52}]$. Therefore, the nominal discrepancy between $\boldsymbol{P}_1$ and $\boldsymbol{P}_2$ is

$$\Delta\boldsymbol{P}=\boldsymbol{P}_1-\boldsymbol{P}_2=f(\boldsymbol{\theta},\boldsymbol{L}_1)-f(\boldsymbol{\theta},\boldsymbol{L}_2) \tag{18}$$

Taking advantage of the measuring instruments, we can obtain the actual discrepancy $\Delta\bar{\boldsymbol{P}}$

$$\Delta\bar{\boldsymbol{P}}=\bar{\boldsymbol{P}}_1-\bar{\boldsymbol{P}}_2=f(\boldsymbol{\theta}+\Delta\boldsymbol{\theta},\boldsymbol{L}_1)-f(\boldsymbol{\theta}+\Delta\boldsymbol{\theta},\boldsymbol{L}_2) \tag{19}$$

where $\bar{\boldsymbol{P}}_1$ is the actual pose of $\boldsymbol{P}_1$, and $\bar{\boldsymbol{P}}_2$ the actual pose of $\boldsymbol{P}_2$. $\Delta\boldsymbol{\theta}=[\Delta\theta_1\ \Delta\theta_2\cdots\ \Delta\theta_{12}]^{\mathrm{T}}$ is the vector of 12 structure parameter errors.

Thus, the difference between $\Delta\boldsymbol{P}$ and $\Delta\bar{\boldsymbol{P}}$ is

$$\Delta\boldsymbol{e}=\Delta\bar{\boldsymbol{P}}-\Delta\boldsymbol{P}=f(\boldsymbol{\theta}+\Delta\boldsymbol{\theta},\boldsymbol{L}_1)-f(\boldsymbol{\theta}+\Delta\boldsymbol{\theta},\boldsymbol{L}_2)-(f(\boldsymbol{\theta},\boldsymbol{L}_1)-f(\boldsymbol{\theta},\boldsymbol{L}_2))=(f(\boldsymbol{\theta}+\Delta\boldsymbol{\theta},\boldsymbol{L}_1)-f(\boldsymbol{\theta},\boldsymbol{L}_1))-(f(\boldsymbol{\theta}+\Delta\boldsymbol{\theta},\boldsymbol{L}_2)-f(\boldsymbol{\theta},\boldsymbol{L}_2)) \tag{20}$$

where $\Delta\boldsymbol{e}=[\Delta e_x\ \Delta e_y\ \Delta e_z\ \Delta e_\alpha\ \Delta e_\beta\ \Delta e_\gamma]^{\mathrm{T}}$ represents the measurement errors in six DOF.

Using Taylor's expansion and removing the high order terms, the following equations are obtained

$$f(\boldsymbol{\theta}+\Delta\boldsymbol{\theta},\boldsymbol{L}_1)-f(\boldsymbol{\theta},\boldsymbol{L}_1)\approx\frac{\partial f(\boldsymbol{\theta},\boldsymbol{L}_1)}{\partial\theta_1}\Delta\theta_1+\frac{\partial f(\theta,L_1)}{\partial\theta_2}\Delta\theta_2+\cdots+\frac{\partial f(\boldsymbol{\theta},\boldsymbol{L}_1)}{\partial\theta_{12}}\Delta\theta_{12}$$

$$f(\boldsymbol{\theta}+\Delta\boldsymbol{\theta},\boldsymbol{L}_2)-f(\boldsymbol{\theta},\boldsymbol{L}_2)\approx\frac{\partial f(\boldsymbol{\theta},\boldsymbol{L}_2)}{\partial\theta_1}\Delta\theta_1+\frac{\partial f(\boldsymbol{\theta},\boldsymbol{L}_2)}{\partial\theta_2}\Delta\theta_2+\cdots+\frac{\partial f(\boldsymbol{\theta},\boldsymbol{L}_2)}{\partial\theta_{12}}\Delta\theta_{12}$$

Hence

$$\Delta\boldsymbol{e}=\frac{\partial f(\boldsymbol{\theta},\boldsymbol{L}_1)}{\partial\theta_1}\Delta\theta_1+\frac{\partial f(\boldsymbol{\theta},\boldsymbol{L}_1)}{\partial\theta_2}\Delta\theta_2+\cdots+\frac{\partial f(\boldsymbol{\theta},\boldsymbol{L}_1)}{\partial\theta_{12}}\Delta\theta_{12}-\left[\frac{\partial f(\boldsymbol{\theta},\boldsymbol{L}_2)}{\partial\theta_1}\Delta\theta_1+\frac{\partial f(\boldsymbol{\theta},\boldsymbol{L}_2)}{\partial\theta_2}\Delta\theta_2+\cdots+\frac{\partial f(\boldsymbol{\theta},\boldsymbol{L}_2)}{\partial\theta_{12}}\Delta\theta_{12}\right]=\left[\frac{\partial f(\boldsymbol{\theta},\boldsymbol{L}_1)}{\partial\theta_1}-\frac{\partial f(\boldsymbol{\theta},\boldsymbol{L}_2)}{\partial\theta_1}\right]\Delta\theta_1+\left[\frac{\partial f(\boldsymbol{\theta},\boldsymbol{L}_1)}{\partial\theta_2}-\frac{\partial f(\boldsymbol{\theta},\boldsymbol{L}_2)}{\partial\theta_2}\right]\Delta\theta_2+\cdots+\left[\frac{\partial f(\boldsymbol{\theta},\boldsymbol{L}_1)}{\partial\theta_{12}}-\frac{\partial f(\boldsymbol{\theta},\boldsymbol{L}_2)}{\partial\theta_{12}}\right]\Delta\theta_{12} \tag{21}$$

Namely

$$\Delta\boldsymbol{e}=\left[\frac{\partial f(\boldsymbol{\theta},\boldsymbol{L}_1)}{\partial\theta_1}-\frac{\partial f(\boldsymbol{\theta},\boldsymbol{L}_2)}{\partial\theta_1}\cdot\frac{\partial f(\boldsymbol{\theta},\boldsymbol{L}_1)}{\partial\theta_2}-\frac{\partial f(\boldsymbol{\theta},\boldsymbol{L}_2)}{\partial\theta_2}\cdots\frac{\partial f(\boldsymbol{\theta},\boldsymbol{L}_1)}{\partial\theta_{12}}-\frac{\partial f(\boldsymbol{\theta},\boldsymbol{L}_2)}{\partial\theta_{12}}\right]\cdot\begin{bmatrix}\Delta\theta_1\\\Delta\theta_2\\\vdots\\\Delta\theta_{12}\end{bmatrix}=\boldsymbol{J}\Delta\boldsymbol{\theta} \tag{22}$$

Eq. (22) can be expanded as follows

$$\begin{bmatrix}\Delta e_x\\\Delta e_y\\\Delta e_z\\\Delta e_\alpha\\\Delta e_\beta\\\Delta e_\gamma\end{bmatrix}=\begin{bmatrix}\frac{\partial f_x(\boldsymbol{\theta},\boldsymbol{L}_1)}{\partial\theta_1}-\frac{\partial f_x(\boldsymbol{\theta},\boldsymbol{L}_2)}{\partial\theta_1} & \frac{\partial f_x(\boldsymbol{\theta},\boldsymbol{L}_1)}{\partial\theta_2}-\frac{\partial f_x(\boldsymbol{\theta},\boldsymbol{L}_2)}{\partial\theta_2} & \cdots & \frac{\partial f_x(\boldsymbol{\theta},\boldsymbol{L}_1)}{\partial\theta_{12}}-\frac{\partial f_x(\boldsymbol{\theta},\boldsymbol{L}_2)}{\partial\theta_{12}}\\ \frac{\partial f_y(\boldsymbol{\theta},\boldsymbol{L}_1)}{\partial\theta_1}-\frac{\partial f_y(\boldsymbol{\theta},\boldsymbol{L}_2)}{\partial\theta_1} & \frac{\partial f_y(\boldsymbol{\theta},\boldsymbol{L}_1)}{\partial\theta_2}-\frac{\partial f_y(\boldsymbol{\theta},\boldsymbol{L}_2)}{\partial\theta_2} & \cdots & \frac{\partial f_y(\boldsymbol{\theta},\boldsymbol{L}_1)}{\partial\theta_{12}}-\frac{\partial f_y(\boldsymbol{\theta},\boldsymbol{L}_2)}{\partial\theta_{12}}\\ \frac{\partial f_z(\boldsymbol{\theta},\boldsymbol{L}_1)}{\partial\theta_1}-\frac{\partial f_z(\boldsymbol{\theta},\boldsymbol{L}_2)}{\partial\theta_1} & \frac{\partial f_z(\boldsymbol{\theta},\boldsymbol{L}_1)}{\partial\theta_2}-\frac{\partial f_z(\boldsymbol{\theta},\boldsymbol{L}_2)}{\partial\theta_2} & \cdots & \frac{\partial f_z(\boldsymbol{\theta},\boldsymbol{L}_1)}{\partial\theta_{12}}-\frac{\partial f_z(\boldsymbol{\theta},\boldsymbol{L}_2)}{\partial\theta_{12}}\\ \frac{\partial f_\alpha(\boldsymbol{\theta},\boldsymbol{L}_1)}{\partial\theta_1}-\frac{\partial f_\alpha(\boldsymbol{\theta},\boldsymbol{L}_2)}{\partial\theta_1} & \frac{\partial f_\alpha(\boldsymbol{\theta},\boldsymbol{L}_1)}{\partial\theta_2}-\frac{\partial f_\alpha(\boldsymbol{\theta},\boldsymbol{L}_2)}{\partial\theta_2} & \cdots & \frac{\partial f_\alpha(\boldsymbol{\theta},\boldsymbol{L}_1)}{\partial\theta_{12}}-\frac{\partial f_\alpha(\boldsymbol{\theta},\boldsymbol{L}_2)}{\partial\theta_{12}}\\ \frac{\partial f_\beta(\boldsymbol{\theta},\boldsymbol{L}_1)}{\partial\theta_1}-\frac{\partial f_\beta(\boldsymbol{\theta},L_2)}{\partial\boldsymbol{\theta}_1} & \frac{\partial f_\beta(\boldsymbol{\theta},\boldsymbol{L}_1)}{\partial\theta_2}-\frac{\partial f_\beta(\boldsymbol{\theta},\boldsymbol{L}_2)}{\partial\theta_2} & \cdots & \frac{\partial f_\beta(\boldsymbol{\theta},\boldsymbol{L}_1)}{\partial\theta_{12}}-\frac{\partial f_\beta(\boldsymbol{\theta},\boldsymbol{L}_2)}{\partial\theta_{12}}\\ \frac{\partial f_\gamma(\boldsymbol{\theta},\boldsymbol{L}_1)}{\partial\theta_1}-\frac{\partial f_\gamma(\boldsymbol{\theta},\boldsymbol{L}_2)}{\partial\theta_1} & \frac{\partial f_\gamma(\boldsymbol{\theta},\boldsymbol{L}_1)}{\partial\theta_2}-\frac{\partial f_\gamma(\boldsymbol{\theta},\boldsymbol{L}_2)}{\partial\theta_2} & \cdots & \frac{\partial f_\gamma(\boldsymbol{\theta},\boldsymbol{L}_1)}{\partial\theta_{12}}-\frac{\partial f_\gamma(\boldsymbol{\theta},\boldsymbol{L}_2)}{\partial\theta_{12}}\end{bmatrix}\begin{bmatrix}\Delta\theta_1\\\Delta\theta_2\\\vdots\\\Delta\theta_{12}\end{bmatrix} \tag{23}$$

After transformation, Eq. (8) can be written as

$$\Delta\boldsymbol{\theta}=\boldsymbol{J}^{-1}\Delta\boldsymbol{e} \tag{24}$$

From Eq. (24), we know that each item of matrix $\boldsymbol{J}$ is the effect of a geometrical parameter error on the output of the tripod machine tool, namely, the sensitivity of parameter error with respect to the output error. Therefore, if we can obtain the error sensitivity matrix $\boldsymbol{J}$ and measure the error data, we can identify the geometrical structure parameter errors of tripod machine tools.

4.2 Error sensitive matrix calculation and identification of the tripod machine tool

Since the closed form solution of the forward kinematics model cannot be obtained, it is very difficult to directly construct the error sensitivity matrix $\boldsymbol{J}$ using partial differential. In practice, we can displace each partial differential in $\boldsymbol{J}$ using the forward difference operator as follows

$$\frac{\partial f_i(\boldsymbol{\theta},\boldsymbol{L}_1)}{\partial \theta_j} \approx f(\theta_1,\theta_2,\cdots,\theta_{j-1},\theta_j+1,\theta_{j+1},\cdots,\theta_{12},\boldsymbol{L}_1)-f(\boldsymbol{\theta},\boldsymbol{L}_1) \tag{25}$$

We certainly also can use the center difference, backward difference, or small step difference instead of the forward difference.

Table 2 is the calculated results of the parameters listed in Table 1, with a ±1 mm step center difference operator, at the location (100,200,−2 100,20,30). Table 3 is the calculated results with a 1 mm step forward difference. Table 4 is the calculated result with a ±0.1 mm step center difference. Since the dimensions of tripod machine tools are much larger than the difference step (see Table 5), the difference of between Tables 2, 3 and 4 is only with in the range of 0.1 μm. Therefore, a 1 mm step can satisfy the needs of the machining and the robot.

Table 2 Results of central difference with a ±1 mm step

Parameter θ	a_1	b	c_1	d_1	d_2	T_2	T_3	d	T_1	c
$\Delta x/\Delta\theta$	−0.635 9	0.922 5	0.484 0	−0.994 8	0.004 8	0.754 2	−0.469 8	0.023 0	0.454 7	0.888 2
$\Delta y/\Delta\theta$	−0.688 0	0.002 1	0.523 6	−0.002 1	−0.002 1	0.432 0	−0.171 0	0.095 1	0.885 5	0.454 7
$\Delta z/\Delta\theta$	0.107 2	0.044 2	−0.081 5	−0.047 7	−0.024 5	−0.494 4	−0.866 0	−0.995 2	0.095 1	0.064 0
$\Delta\alpha/\Delta\theta$	0.020 0	0.013 4	−0.015 2	−0.014 6	−0.014 6	0	0	0	0	0
$\Delta\beta/\Delta\theta$	0.022 6	−0.023 9	−0.017 2	0.025 8	0.025 8	0	0	0	0	0

Table 3 Results of the forward difference with a 1 mm step

Parameter θ	a_1	b	c_1	d_1	$d2$	r	l	d	t	c
$\Delta x/\Delta\theta$	−0.636 0	0.922 3	0.483 4	−0.993 6	0.006 0	0.754 2	−0.469 8	0.023 0	0.454 7	0.888 2
$\Delta y/\Delta\theta$	−0.688 1	0.002 1	0.523 0	−0.002 1	−0.00 21	0.432 0	−0.171 0	0.095 1	0.885 5	0.454 7
$\Delta z/\Delta\theta$	0.107 4	0.044 4	−0.081 3	−0.047 4	−0.024 7	−0.494 4	−0.866 0	−0.995 2	0.095 1	0.064 0
$\Delta\alpha/\Delta\theta$	0.020 0	0.013 5	−0.015 2	−0.014 6	−0.014 6	0	0	0	0	0
$\Delta\beta/\Delta\theta$	0.022 6	−0.023 9	−0.017 2	0.025 7	0.0257 7	0	0	0	0	0

Table 4 Results of the central difference with a ±0.1 mm step

Parameter θ	a_1	b	c_1	d_1	d_2	r	l	d	t	c
$\Delta x/\Delta\theta$	−0.635 9	0.922 5	0.484 0	−0.994 8	0.004 8	0.754 2	−0.469 8	0.023 0	0.454 7	0.888 2
$\Delta y/\Delta\theta$	−0.688 0	0.002 1	0.523 6	−0.002 1	−0.002 1	0.432 0	−0.171 0	0.095 1	0.885 5	0.454 7
$\Delta z/\Delta\theta$	0.107 2	0.044 2	−0.081 5	−0.047 7	−0.024 5	−0.494 4	−0.866 0	−0.995 2	0.095 1	0.064 0
$\Delta\alpha/\Delta\theta$	0.020 0	0.013 4	−0.015 2	−0.014 6	−0.014 6	0	0	0	0	0
$\Delta\beta/\Delta\theta$	0.022 6	−0.023 9	−0.017 2	0.025 8	0.025 80	0	0	0	0	0

In a measurement, the data in $\Delta\boldsymbol{e}$ are probably not sufficient to identify 12 structural parameters. To obtain better results, it is necessary to measure more data in different directions and different spatial locations. We can establish a series of error sensitivity matrices $\boldsymbol{J}_1,\boldsymbol{J}_2,\cdots,\boldsymbol{J}_n$ and its corresponding measurement errors $\Delta\boldsymbol{e}_1,\Delta\boldsymbol{e}_2,\cdots,\Delta\boldsymbol{e}_n$. As a result, we can establish the equations

$$\begin{bmatrix}\Delta\boldsymbol{e}_1\\ \Delta\boldsymbol{e}_2\\ \vdots\\ \Delta\boldsymbol{e}_n\end{bmatrix}=\begin{bmatrix}\boldsymbol{J}_1\\ \boldsymbol{J}_2\\ \vdots\\ \boldsymbol{J}_n\end{bmatrix}\Delta\boldsymbol{\theta}$$

To solve the above equations, we establish a target function: $\min F=\|\Delta\boldsymbol{e}-\boldsymbol{J}\Delta\boldsymbol{\theta}\|$, and adopt an optimization method to solve it. Finally, the geometrical parameter errors of tripod machine tools can be obtained with the identification method.

5 Application

To validate the identification method, an experiment was performed on LINKS-EXE700 tripod machine tools, shown in Fig. 4. The machine tool was made by Harbin Measuring & Cutting Tool Group Co. Ltd. in China. The nominal geometrical structure parameters of the machine tool are shown in Table 5.

Table 5 Initial parameter values and correction results of the tripod platform mm

Parameter	a_1	a_2	b	c_1	c_2	d_1	d_2	t_2	t_3	d	c	t_1
Nominal value	620	620	670	195	195	195	50	120	270	470	50	0
Amendatory value	−0.094	1.825	−0.710	−0.332	−2.249	1.459	−0.822	1.177	1.736	0.534	0.367	−1.347

Fig. 4 LINKS-EXE700 tripod machine tool

Before calibration, the error data of the tripod machine tool must be measured. In the measurement process, the following matters must be addressed:

(1) To avoid only obtaining good accuracy in the local workspace of the machine tools, measurement data should cover the whole workspace of tripod machine tools.

(2) If some accuracy of the geometrical structural parameters can be guaranteed in the process of manufacturing and installation, other parameters can be identified. As a result, the corresponding measurement data and error sensitivity matrix can be reduced.

(3) As known from the identification model, if a high identification precision of tripod machine tools is to be demanded, the initial errors of the mechanism should not be too large. Otherwise, the identification requires multiple calibrations.

In the experiment, as shown in Fig. 5, we moved the machine to 20 different distances along different directions and measured the actual moving distances of the machine using a laser tracker. Thus, the error matrix was built with the error between the measured moving distances and the specified moving distances. Finally, according to the equation $\min F = \Delta \boldsymbol{e} - \boldsymbol{J}\Delta\boldsymbol{\theta}$, the correct results were calculated using the least square optimization method. The results of the measurement error, residual error and amendatory error are shown in Table 6. The amendatory values of geometrical structure parameters are shown in Table 5.

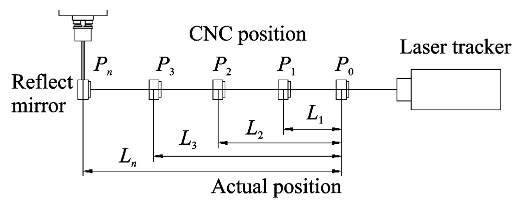

Fig. 5 Measure error data

Table 6 Results of measurement error and residual error mm

Data series	Measurement error	Residual error	Amendatory
1	−0.275 08	0.007 703	−0.282 78
2	0.576 227	−0.186 78	0.763 007
3	0.560 592	0.075 646	0.484 945
4	0.168 512	0.008 371	0.160 141
5	−0.366 5	0.186 346	−0.552 84
6	−0.956 89	0.142 164	−1.099 05
7	0.119 681	0.219 224	−0.099 54
8	−0.398 36	0.124 183	−0.522 55
9	0.439 41	−0.000 89	0.440 303
10	0.480 904	−0.236 32	0.717 226
11	−0.426 76	−0.076 11	−0.350 65
12	0.601 641	−0.206 4	0.808 043
13	0.792 223	−0.056 74	0.848 965
14	0.097 527	−0.070 99	0.168 514
15	0.384 017	−0.179 56	0.563 575
16	0.887 463	−0.105 67	0.993134
17	0.098 316	0.195 827	−0.097 51
18	0.456 774	0.000 23	0.456 543
19	0.076 758	4.99×10^{-5}	0.076 708
20	−0.474 14	0.207 729	−0.681 87

Fig. 6 shows the plot of the calibration results. The measurement error range of the tripod machine tool is [−0.956, 0.792], and the residual error range is [−0.236, 0.219]. The absolute error of the tripod machine tool is reduced from 1.74 mm to 0.44 mm.

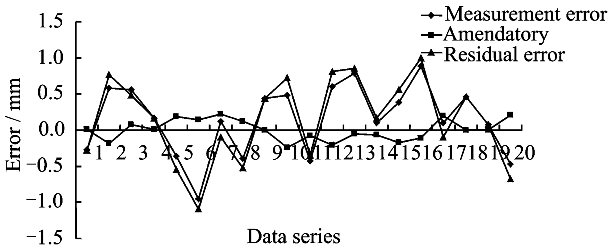

Fig. 6 Results of measurement error and residual error

6 Conclusions

Structure and pose description method of tripod machine tools was introduced, and the kinematics model was analyzed. An identification method for the tripod machine tool was presented and implemented. The proposed method was validated by an experiment. The following conclusions can be drawn.

(1) The parameter error sensitivity matrix represents the structure parameter errors with respect to the output error of tripod machine tools. Taking advantage of the matrix, the parameters of tripod machine tool can be identified.

(2) Since the partial differential of the kinematics model cannot be directly obtained, the error sensitivity matrix of the tripod machine tool can be created using a numerical method. To accurately identify the parameters of the tripod machine tool, a group of error sensitivity matrices and measurement data are built, and the parameters can be calculated using an optimization method.

(3) The method can also be used for identifying parameters of other non-linear systems using an explicit mathematical model.

References:

[1] Majarena A C, Santolaria J, Samper D, et al. An overview of kinematic and calibration models using internal/external sensors or constraints to improve the behavior of spatial parallel mechanisms[J]. Sensors, 2010, 11 (10): 10256-10297.

[2] Hesselbach J, Bier C, Pietsch I, et al. Passive-joint sensors for parallel robots[J]. Mechatronics, 2005, 15(1):43-65.

[3] Gao Jianshe, Cheng Li, Zhao Yongsheng. Kinetic self-calibration of novel 5-DOF parallel machine tool[J]. Computer Integrated Manufacturing Systems, 2007, 13 (4):738-743. (in Chinese)

[4] Ren X D, Feng Z R, Su C P. A new calibration method for parallel kinematics machine tools using orientation constraint[J]. Int J Mach Tools Manuf, 2009, 49(9):708-729.

[5] Chiang M H, Lin H T, Hou C L, Development of a stereo vision measurement system for a 3D three-axial pneumatic parallel mechanism robot arm[J]. Sensors, 2011, 11(2):2257-2281.

[6] Daney D. Kinematic calibration of the Gough platform[J]. Robotica, 2003, 21(6):677-690.

[7] Trapet E, Savio E, de Chiffre L. New advances in traceability of CMMs for almost the entire range of industrial dimensional metrology needs CIRP[J]. Ann Manuf Technol, 2004, 53(1):4330- 4338.

[8] Majarena A C, Santolaria J, Samper D, et al Modelling and calibration of parallel mechanisms using linear optical sensorsand a coordinate measuring machine [J]. Meas Sci Technol, 2011, 22(10):1-12.

[9] Zhong Shisheng, Yang Xiaojun, Wang Zhixing. Research on calibration method based on 6-TPS type parallel machine tool[J]. Computer Integrated Manufacturing Systems, 2005, 11(10):1069-1074.

[10] Gao Meng, Li Tiemin, Ye Peiqing, et al. Precision evaluation oriented parameter identification of PKM tools[J]. Chinese Journal of Mechanical Engineering, 2005, 41(5):79-84. (in Chinese)

[11] Wei Shimin, Zhou Xiaoguang, Liao Qizheng. Research on the kinematics calibration of six-axes parallel maehine tool[J]. China Mechanical Engineering, 2003, 14(23):1981-1986. (in Chinese)

[12] Liu Wentao, Tang Dewei, Wang Zhixing. Cocktail method for Stewart platform calibration[J]. Chinese Journal of Mechanical Engineering, 2004, 40(12): 48-53. (in Chinese)

[13] Yung Ting, Jar H C, Li C C. Measurement and calibration for Stewart micro-manipulation system[J]. Precision Engineering, 2007, 31(3):226-233.

(Executive Editor: Zhang Bei)